

# Correlation of macroscopic instability and Lyapunov times in the general three-body problem

Seppo Mikkola<sup>1,2\*</sup> and Kiyotaka Tanikawa<sup>2†</sup>

<sup>1</sup>Tuorla Observatory, University of Turku, Väisäläntie 20, Piikkiö, Finland

<sup>2</sup>National Astronomical Observatory of Japan, Mitaka, Tokyo 181-8588, Japan.

23 October 2021

## ABSTRACT

We conducted extensive numerical experiments of equal mass three-body systems until they became disrupted. The system lifetimes, as a bound triple, and the Lyapunov times show a correlation similar to what has been earlier obtained for small bodies in the Solar System. Numerical integrations of several sets of differently randomised initial conditions produced the same relationship of the instability time and Lyapunov time. Marginal probability densities of the various times in the three-body experiments are also discussed. Our high accuracy numerical method for three-body orbit computations and Lyapunov time determinations is concisely described.

**Key words:** stellar dynamics – methods:  $N$ -body simulations – celestial mechanics

## 1 INTRODUCTION

Lecar, Franklin, & Murison (1992) first suggested the existence of a relationship between the local Lyapunov time and a survival time of the orbit of an asteroid in the Solar System. They gave numerical evidence of a powerlaw relation

$$\frac{t_d}{t_0} = A \left( \frac{t_e}{t_0} \right)^n, \quad (1)$$

where  $t_d$  is the survival time,  $t_e$  the local Lyapunov time [which is defined as the inverse of the mean time derivative of the logarithm of the variational equation solution during the interplay period of the system] and  $t_0$  some normalisation time. For the powerlaw index they estimated the value  $n \approx 1.8$ . The relation is by no means an exact one but rather the equation fits the centre of a scatter diagram of the logarithms of the times. The relation have been studied by several authors but mainly for asteroid motions and for some artificial mappings. Additional discussion can be found e.g. in Murison, Lecar, & Franklin (1994) and Lecar et al. (2001). Morbidelli & Froeschlé (1996) discovered two separate regions: the Nekhoroshev region in which the survival times are exponentially long, and resonance overlap region in which an expression like Eq.(1) more accurately apply. However, they were unable to provide any theoretical explanation. Later Murray & Holman (1997) obtained evidence against the generality of the ‘law’ (1).

In this paper we present evidence for a relation of the power law type in the general equal mass three-body problem.

## 2 PROBLEM AND DEFINITIONS

The problem studied in this paper is the relationship between lifetimes and Lyapunov times of a three-body system.

The lifetime is defined as the duration of the numerical experiment to the point when the system ejects one particle. The criterion used was: the single particle is moving away in a hyperbolic relative orbit at a distance  $> 50$  times the semi-major-axis of the surviving binary. Then, using the orbital elements, we compute the (formal) time of pericentre passage for this relative hyperbola. This time, symbol  $t_d$ , is then considered to be the moment of disruption.

In the strict mathematical sense the Lyapunov time does not exist for unstable triples, because after the systems disrupt they become essentially quasi-periodic. We can still use the variational equations solutions to measure the sensitivity of the system with respect to variations of initial conditions. If the system behaves chaotically, then  $\delta\mathbf{r}(t)$ , the solution of the variational equations, has the order of magnitude  $|\delta\mathbf{r}(t)| \sim \exp(t/t_e)$ . Evaluating this at the time  $t = t_d$  and solving for  $t_e$  gives (formally) a Lyapunov time as

$$t_e = t_d / \ln |\delta\mathbf{r}(t_d)|. \quad (2)$$

Writing the above in another way, one notes that the quantity

$$Z = \ln |\delta\mathbf{r}(t_d)| = t_d/t_e, \quad (3)$$

i.e. the logarithm of the variation at the moment of disruption, is actually the lifetime in units of the Lyapunov time.

\* E-mail: seppo.mikkola@utu.fi

† E-mail: tanikawa.ky@nao.ac.jp

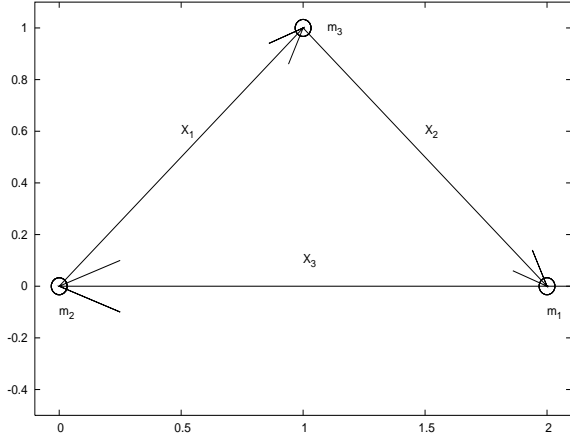


Figure 1. Labelling of vectors in the three-body regularization.

### 3 NUMERICAL METHOD

Our numerical method is based on the logarithmic Hamiltonian (Mikkola & Tanikawa (1999a,b); Preto & Tremaine (1999); Mikkola (2006)) which, with the leapfrog algorithm, gives regular results. Instead of centre-of-mass coordinates we use the three interparticle vectors (see Figure 1)

$$\mathbf{X}_1 = \mathbf{r}_3 - \mathbf{r}_2; \quad \mathbf{X}_2 = \mathbf{r}_1 - \mathbf{r}_3; \quad \mathbf{X}_3 = \mathbf{r}_2 - \mathbf{r}_1. \quad (4)$$

as new coordinates. Let the corresponding velocities be  $\mathbf{V}_k = \dot{\mathbf{X}}_k$ , then the centre-of-mass kinetic and potential energies can be written

$$T = \frac{1}{4M} \sum_{i < j} m_i m_j \mathbf{V}_{k_{ij}}^2; \quad U = \sum_{i < j} \frac{m_i m_j}{|\mathbf{X}_{k_{ij}}|}, \quad (5)$$

where  $M = \sum_k m_k$  is the total mass and  $k_{ij} = 6 - i - j$ .

The equations of motion are

$$\dot{\mathbf{X}}_k = \mathbf{V}_k; \quad \dot{\mathbf{V}}_k = -M \frac{\mathbf{X}_k}{|\mathbf{X}_k|^3} + m_k \sum_{\nu} \frac{\mathbf{X}_{\nu}}{|\mathbf{X}_{\nu}|^3}. \quad (6)$$

and after the application of the logarithmic Hamiltonian modification they read

$$t' = 1/(T + B); \quad \mathbf{X}'_k = \dot{\mathbf{X}}_k/(T + B); \quad \mathbf{V}'_k = \dot{\mathbf{V}}_k/U. \quad (7)$$

where the constant  $B = U - T$  is the negative of energy. The leapfrog algorithm is now possible since the right hand sides in these equations do not depend on the left hand side variable.

To obtain the solutions to the variational equations  $\delta \mathbf{X}, \delta t, \delta \mathbf{V}$  we first wrote the code to compute the motion and then differentiated that line by line (i.e. adding the (analytical) code lines for the differentials), thus obtaining precise differentials of the numerical algorithm used. The results are then in the time transformed system in which time also has a variation. The transformation to physical system is simple: If we denote the physical system variations with  $\Delta$ , we can write for any quantity  $f$  the equation

$$\Delta f = \delta f - \delta t \dot{f}, \quad (8)$$

which gives the desired result.

Leapfrog is used only as a basic method and the results are improved to high precision by means of the extrapolation method (Bulirsch and Stoer (1966)).

The usage of the relative vectors, instead of some inertial coordinates, is advantageous in attempting to avoid large round-

off effects. One could also integrate only two of the triangle sides, obtaining the remaining one from the conditions  $\sum_k \mathbf{X}_k = \mathbf{0}$ ;  $\sum_k \mathbf{V}_k = \mathbf{0}$ . This would hardly reduce the computational effort required by the method. Instead one may, occasionally, compute the longest side, and the corresponding velocity, from the above triangle conditions. Note that the sums of the sides are not only integrals of the exact solution, but they are also exactly conserved by the leapfrog mapping. On the other hand, the extrapolation procedure does not necessarily conserve this relation.

The transformation from the variables  $\mathbf{X}$  to centre-of-mass coordinates  $\mathbf{r}$  can be done as

$$\begin{aligned} \mathbf{r}_1 &= \frac{(m_3 \mathbf{X}_2 - m_2 \mathbf{X}_3)}{M} \\ \mathbf{r}_2 &= \frac{(m_1 \mathbf{X}_3 - m_3 \mathbf{X}_1)}{M} \\ \mathbf{r}_3 &= \frac{(m_2 \mathbf{X}_1 - m_1 \mathbf{X}_2)}{M}, \end{aligned} \quad (9)$$

and the velocities obey the same rule.

### 4 INITIAL CONDITIONS

The systems we studied were equal mass systems. We set all the masses  $m_k = 1$  (also the gravitational constant was chosen to be  $G = 1$ ).

We attempted to produce random initial conditions although it is not clear how it should be done since the phase space is infinite. Initial experiments with various ways showed that the results considered in this paper do not depend much on how the initial values are randomised. We finally chose the following algorithm:

First we selected all the 9 coordinates  $x_k$  from a uniform distribution inside a 9 dimensional sphere and similarly the velocity components  $v_k$ . Those were reduced to centre-of-mass system and scaling factors  $c_r$  and  $c_v$  for the coordinates and velocities respectively were determined from the conditions

$$E = -1, \quad \text{and} \quad T/U = k, \quad (10)$$

where  $T, U$  and  $E = T - U$  are the kinetic energy, potential and total energy respectively, and  $k$ , the virial ratio, is a selected quantity. After obtaining the scaling coefficients we simply replace

$$x_{\mu} \rightarrow c_r x_{\mu}, \quad v_{\mu} \rightarrow c_v v_{\mu}, \quad \mu = 1, \dots, 9 \quad (11)$$

We considered the three values  $k = 0, k = 0.1$  and  $k = 0.5$ . The first one thus gave a system starting at rest (often called ‘the free-fall problem’) and thus being a plane problem with zero angular momentum. The second value  $k = 0.1$  gives systems with small initial velocities and the value  $k = 0.5$  corresponds to systems starting at the state of virial equilibrium although here it only means larger initial velocities and non-negligible angular momentum.

## 5 RESULTS

### 5.1 Experiments

We conducted 10,000 experiments for each value of the initial virial coefficient  $k = 0, 0.1, 0.5$ . Thus altogether 30,000 simulations were run to the point when the system disrupted, or the system time exceeded 100,000 time units. There were only 383 cases in which the computation was halted because of exceeding the time limit. There was no reason to halt any of the experiments due to

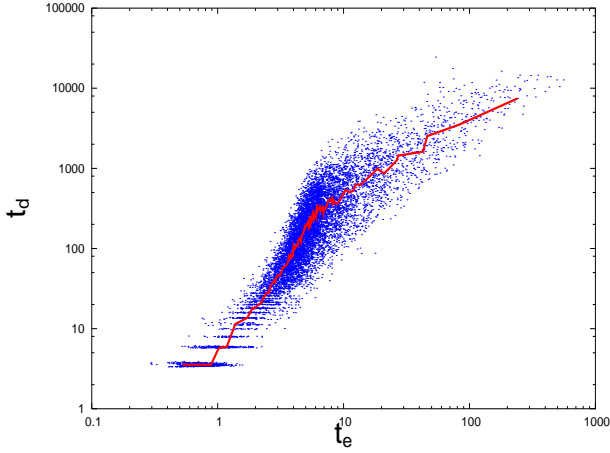


**Figure 2.** The scatter diagram of disruption times ( $t_d$ ) and Lyapunov times ( $t_e$ ) for the free-fall experiments. The line is a median line determined such that there are equally many dots under and above the curve at every value of  $t_e$ . Some systematic initial value effects are visible at small times.

loss of accuracy. Our measure of accuracy, the ratio of energy error  $\delta E$  and the Lagrangian  $L = T + U$  satisfied

$$|\delta E|/L < 1.36 \cdot 10^{-11}, \quad (12)$$

in all cases (the number quoted is the maximum), while most values (in 24350 cases) were less than  $10^{-13}$ .

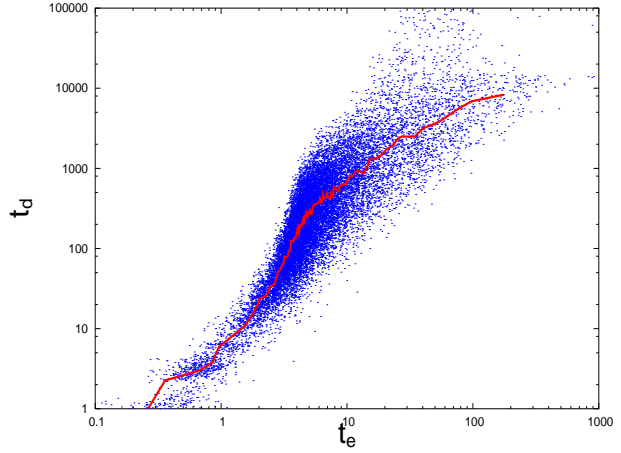
## 5.2 Scatter diagrams

Figure 2 illustrates the scatter diagram of  $(t_e, t_d)$  (times according to Eq.(2)) in logarithmic scale for the free-fall experiments. The line shown is a median produced by sorting the results according to  $t_e$ , then dividing the whole range into 50 intervals each containing equally many cases for which the median was determined by sorting this group according to the disruption times  $t_d$ .

Similarly, Figure 3 illustrates the  $(t_e, t_d)$  scatter diagram of all the other experiments. The similarity is obvious although the scatter is somewhat larger.

A third way of illustrating the correlation of  $(t_e, t_d)$  is given in Figure 4 where the medians are plotted in the same figure. Since in Figures 2 and 3 most cases are concentrated in a much narrower region than the total scale, we restricted this figure into the interval  $.94 < t_e < 35.2$ . These limits were determined such that 5% of the cases are in the region  $t_e < .94$  and similarly 5% in the region  $t_e > 35.2$ . Thus a majority (90%) of data are included in the shown interval. Another reason for this restriction is that, at small times, the systems disrupt almost immediately and the results are likely to be affected by initial value selection. The largest times are affected by long ejections without escape, an effect that may also partly result from initial value sampling.

Here three different median curves are produced: one for the free-fall experiments, one for small and medium angular momentum and one for large angular momentum. These were produced by sorting the experiments according to the angular momentum value, the smaller half of these were included into the small and medium group and the rest were considered to have large angular momentum. One can see that the large angular momentum curve is somewhat above the others, but the difference is minor. The straight line in the figure represents the relation  $t_d = 10t_e^{1.8}$ , which roughly fits the general trend in this region which contains 90% of the data. On



**Figure 3.** The scatter diagram of disruption times ( $t_d$ ) and Lyapunov times ( $t_e$ ) with the median line.

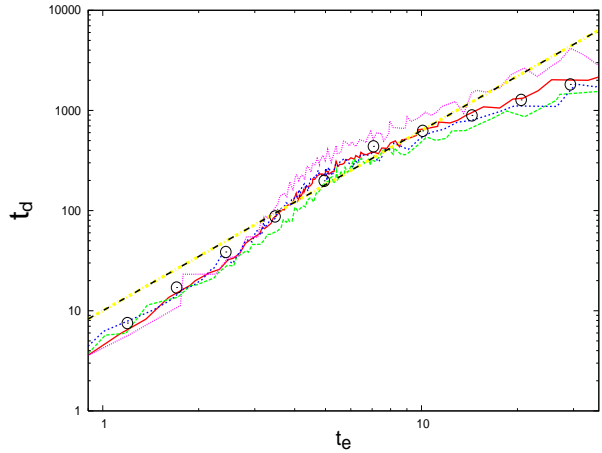


**Figure 4.** Median lines for zero, small and large angular momentum systems. The straight line is for  $t_d = 10 t_e^{1.8}$  and the circles for  $t_e = \min(5t_e^{2.3}, 62t_e)$ . The curve above others is for the large angular momentum experiments. The two others, for zero and small angular momentum, do not differ noticeably.

the other hand, the median curves could be better fitted with two lines: one with  $t_d \approx 5t_e^{2.3}$  for  $t_e < 6$  and with  $t_d \approx 62t_e$  for  $t_e > 6$ , i.e. for large times  $t_d \propto t_e$  (circles in the figure).

## 5.3 Marginal distributions

It may be of some interest to see what are the marginal distributions of the various quantities studied here. We found that, for large values of the times, both  $t_d$  and  $Z = \ln |\delta r| = t_d/t_e$  have exponential probability densities which are approximately given by

$$\psi(t_d) \approx \alpha \exp(-\alpha t_d), \quad \alpha = 1/250 \quad (13)$$

$$\psi(Z) \approx \beta \exp(-\beta Z), \quad \beta = 1/45. \quad (14)$$

These results are illustrated in the Figures 5 and 6. If one assumes those approximations to be valid for small values also then it is easy to derive the probability density for  $t_e$  as

$$\begin{aligned} \psi(t_e) &= \int \delta(t_e - t_d/Z) \alpha \exp(-\alpha t_d) \beta \exp(-\beta Z) dt_d dZ \\ &= \alpha\beta / (\alpha t_e + \beta)^2, \end{aligned} \quad (15)$$

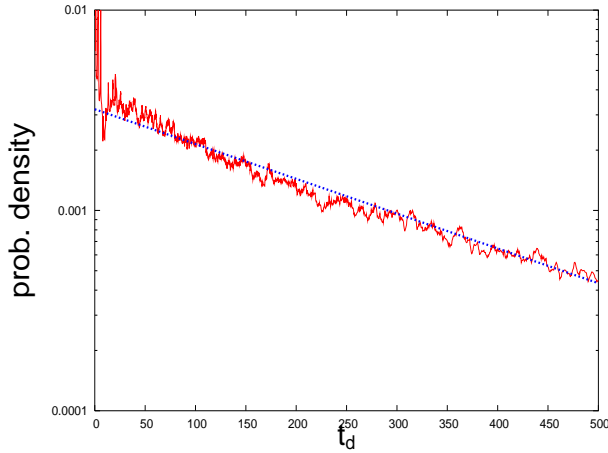


**Figure 5.** Probability density of the disruption times. The line represents the function  $\alpha \exp(-\alpha t_d)$  with  $\alpha = 1/250$

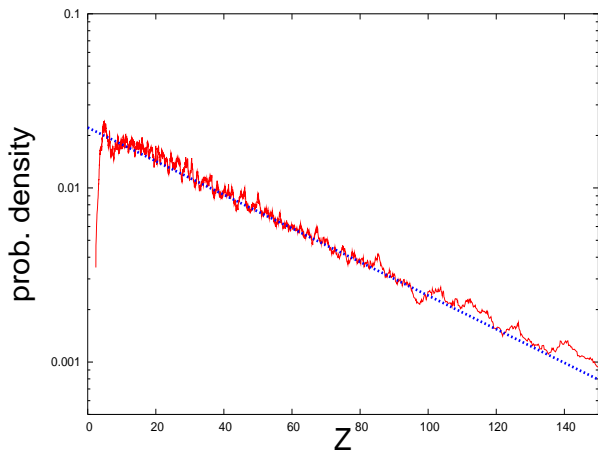


**Figure 6.** Probability density of  $Z = t_d/t_e$  i.e. the disruption time in units of the Lyapunov time. The line drawn represents  $\beta \exp(-\beta Z)$  with  $\beta = 1/45$ .

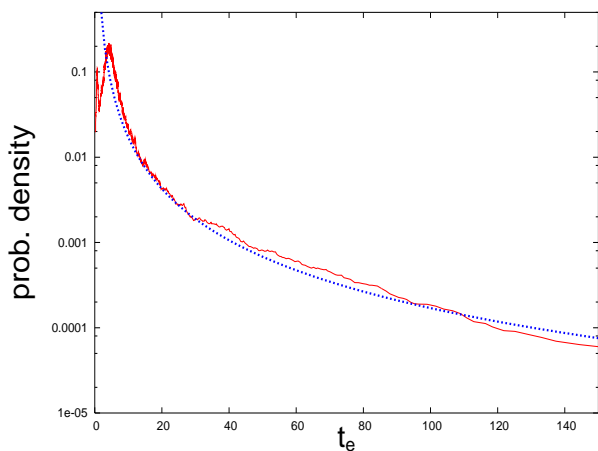


**Figure 7.** Probability density of the Lyapunov times  $t_e$ . This density is clearly not exponential but, for large  $t_e$ , is close to the function  $1.8/t_e^2$  drawn in the figure.

which is qualitatively right, as can be seen from Figure 7, where the probability density of  $t_e$  is illustrated. Numerically this result is not quite correct, presumably because the exponential functions for the probability densities of  $t_d$  and  $Z$  are only valid for large values.

## 6 CONCLUSION

The main result in this investigation is the obvious existence of a relation of the Lecar-Franklin-Murison type in the general equal mass three-body problem. In the region where most (90%) of the cases in our diagram are located the median disruption time can be rather well approximated by a power law of exponent  $n \approx 1.8$  which happens to be close to what Lecar, Franklin, & Murison (1992) obtained in their pioneering paper. This is somewhat surprising since the systems are totally different. On the other hand, our results could also be interpreted in the way that for  $t_e < 6$  the exponent is  $n \approx 2.3$  and for larger  $t_e$  the exponent is simply  $n \approx 1$ . If this is the case, one can conclude that for large  $t_e$ , i.e. for weakly chaotic systems, the disruption time is typically proportional to the Lyapunov time.

Lecar et al. (2001) suggested that the relation in Eq.(1) is valid in Solar System in regions where there are overlapping mean motion resonances. However, in the equal mass three-body problem there are hardly any resonances causing the behaviour, thus the phenomenon may be more directly related to chaos than to resonances. Like Morbidelli & Froeschlé (1996), we too do not have any theoretical explanation for this phenomenon, which seems to be more common than expected.

In addition to the above, it is interesting to note that (for large times) the system lifetimes  $t_d$  have exponential probability density both when measured directly in terms of the systems dynamical time and also when measured in units of the Lyapunov time  $t_e$ . A consequence of this is that the Lyapunov times have a different probability density  $\psi(t_e) \propto t_e^{-2}$ . It would be most interesting to find a theoretical explanation for these facts, but we are unable to provide one.

## REFERENCES

- Bulirsch, R. and Stoer, J., 1966, *Num. Math.*, 8, 1
- Lecar M., Franklin F., Murison M., 1992, *AJ*, 104, 1230
- Lecar M., Franklin F. A., Holman M. J., Murray N. J., 2001, *ARA&A*, 39, 581
- Mikkola S., Tanikawa K., 1999a, *CeMDA*, 74, 287
- Mikkola S., Tanikawa K., 1999b, *MNRAS*, 310, 745
- Mikkola, S., 2006, in *Few-Body Problem: Theory and Computer Simulations, Annales Universitatis Turkuensis. Series 1A, Vol. 358, 2006, C.Flynn, ed.* pp.114–121
- Morbidelli A., Froeschlé C., 1996, *CeMDA*, 63, 227
- Murison M. A., Lecar M., Franklin F. A., 1994, *AJ*, 108, 2323
- Murray N., Holman M., 1997, *AJ*, 114, 1246
- Preto M., Tremaine S., 1999, *AJ*, 118, 2532